Advanced Composite Materials
Publication details, including instructions for authors and subscription information:
http://www.tandfonline.com/loi/tacm20

Applications of carbon-carbon composites to an engine for a future space vehicle

Hiroshi Hatta , Ken Goto , T. Sato & N. Tanatsugu

Version of record first published: 02 Apr 2012.

To cite this article: Hiroshi Hatta , Ken Goto , T. Sato & N. Tanatsugu (2003): Applications of carbon-carbon composites to an engine for a future space vehicle , Advanced Composite Materials, 12:2-3, 237-259

To link to this article: http://dx.doi.org/10.1163/156855103772658588

Adv. Composite Mater., Vol. 12, No. 2-3, pp. 237–259 (2003)

Also available online - www.vsppub.com

Applications of carbon-carbon composites to an engine for a future space vehicle

HIROSHI HATTA *, KEN GOTO, T. SATO and N. TANATSUGU

Institute of Space and Astronautical Science, 3-1-1 Yoshinodai, Sagamihara, Kanagawa 229-8510, Japan

Received 15 July 2002; accepted 20 December 2002

Abstract—Feasibility studies were carried out aiming at the application of carbon/carbon (C/C) composites to a turbine disk, heat exchangers, and a plug nozzle for an engine intended for use in a future reusable space vehicle. In these applications, the maximum temperature was estimated to be about 1500°C. In order to withstand this high temperature, attempts were made to utilize three-dimensionally reinforced C/C composites. The most serious problem encountered in the application of C/Cs to the turbine disk was the loss of fragments of the composite located near the outer periphery due to strong centrifugal force, which resulted in severe vibration due to rotational imbalance. The heat exchangers and plug nozzle have complex shapes in order to realize a large heat exchanging area. Joined structures were explored for these components. The principal effort in these applications has been placed on finding structures requiring low joining strength and developing materials with low gas leakage.

Keywords: Carbon/carbon (C/C) composite; thermo-mechanical properties; turbine blade; heat exchangers; high temperature properties; bonding; gas leakage.

1. INTRODUCTION

Carbon-carbon (C/C) composites are attractive materials because of their superior specific strength and specific elastic modulus at elevated temperatures over 2000°C [1–3]. In light of these advantages, many attempts have been made to apply C/C composites to high temperature structures such as space vehicles, hypersonic airplanes, and fusion reactors [1–7]. However, C/C composites have seldom been applied to primary structures requiring high load bearing capability, mainly due to their weakness against high temperature oxidation. Thus, the improvement of oxidation resistance has been a primary research focus for C/C composites [1–4, 8–13]. As a result, reliable short-term oxidation protection for several

*To whom correspondence should be addressed. E-mail: hatta@pub.isas.ac.jp

hours, and up to about 1500°C is now guaranteed by the combination of a SiC coating and glass crack sealant, but long-term and high temperature resistance is still under active study [4, 8]. In addition to this shortcoming, few reliable mechanical design data for C/C composites are available [1–4]. Consequently, intensive projects have been proposed, for example in the United States, Europe, and Japan for the development of reusable space planes using high temperature composites [14–17], but none of the projects has succeeded, partly due to the difficulty dealing with the high temperature materials.

In spite of the above difficulties, owing to this material's excellent performance at high temperatures, development studies are underway on the applications of C/C composites to a turbine disk, heat exchangers, and plug nozzle for a future spacecraft engine, an air turbo ramjet with an expander cycle, ATREX, engine [17–19]. This engine has been studied for about 15 years at the Institute of Space and Astronautical Science (Japan) as a suitable candidate for the first stage engine of a two-stage-to-orbit, TSTO, space plane. This engine is expected to have sufficient thrust to attain a flight speed of Mach 6 up to an altitude of 35 km. This is a combined cycle engine performing like a turbojet up to Mach 2 flight and a fan-boost ramjet up to Mach 6. Figure 1 shows the schematics of the ATREX engine under development along with its temperature environments. The main features of this engine include the utilization of hydrogen fuel, adoption of an expander cycle to improve high speed capability, and the employment of high temperature composites, especially C/C composites. In the present paper, the design concepts of the turbine disk, heat exchanger, and plug nozzle for the ATREX engine using 3D-C/C composites and the difficulties encountered in its developmental studies are reviewed.

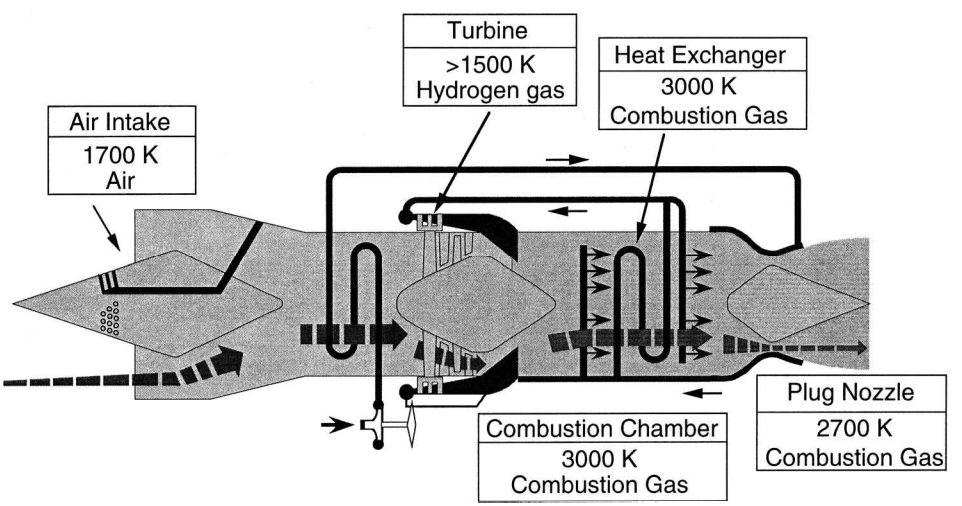

Figure 1. Schematic drawing illustrating the mechanism of an air turbo ramjet engine for use in a future Japanese space vehicle and its temperature environment.

2. CARBON-CARBON COMPOSITES

In addition to their superior mechanical performance at high temperatures, C/C composites have several advantages over other materials, though the C/C composites have a serious drawback of extremely low oxidation resistance. For the turbine application, their low density, low thermal expansion coefficient, and high thermal conductivity are also useful properties regarding thermal stress reduction and the prevention of thermal shock damage. The thermo-mechanical properties of carbon-carbon composites are briefly summarized below for the convenience of later discussion.

2.1. Mechanical properties

The tensile strength of C/C composites generally increases with increasing temperatures up to about 2500°C as shown in Fig. 2 [3, 20, 21], although Young's modulus gradually decreases from about 1500°C. This tendency was also confirmed in other strength, shear and compressive strengths and fracture toughness [22–27]. Hence, we can conservatively estimate the applicability of C/C composites to high temperature structures based on their room temperature properties. The strength of the C/C composite shown in this figure is not high enough for use in the turbine disk of the ATREX engine. For this application, a high strength of about 700 MPa is required for a C/C to guarantee sufficient reliability. The tensile strength of C/C composites is known to be primarily controlled by the strength of fiber/matrix interfaces [21, 29, 30]. By lowering the interfacial strength, the tensile strength of three-dimensionally reinforced C/C composites, 3D-C/Cs, can easily attain the above value [31]. However, it should be noted in the design of C/C structures that the

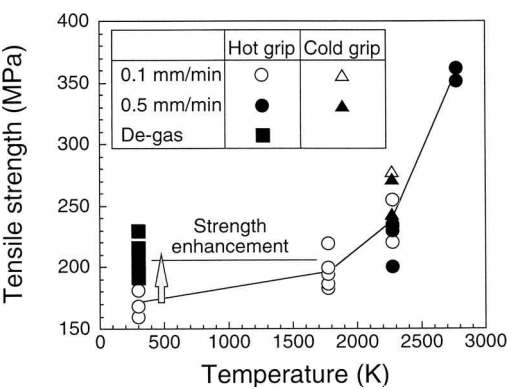

Figure 2. Temperature dependence of tensile strength in a cross-ply-laminated C/C composite obtained under a vacuum up to 2273 K and an Ar atmosphere over it [20]. The difference between C/C strengths with and without de-gas treatment represents the effect of absorbed water. The de-gas treatment was made at 1473 K under a vacuum. The strength improvement up to 2073 K was caused by the evaporation of absorbed gas, while the improvement over 2073 was due to creep deformation.

interfacial degradation simultaneously leads to low compressive strength [32, 33] and low shear strength [34, 35].

Extremely low shear strength is a well-known drawback of C/C composites [36–38]. In particular, interlaminar shear strength (ILSS) is about one-tenth of that of fiber-reinforced plastics; the ILSSs of unidirectional and cross-ply CC composites have been reported to be 20–30 MPa and 10–20 MPa, respectively [22–24, 26, 27, 36]. In their applications to the turbine disk, heat exchangers, and nozzle, complex tri-axial stress distributions are anticipated. In order to avoid premature shear damage, three-dimensionally reinforced, 3D-C/Cs were chosen for ATREX applications [39]. An additional advantage of the 3D-C/Cs is that their fracture toughness is extremely high compared with 2-dimensionally (2D) reinforced C/Cs [40, 41]. This high toughness is derived from the lower interfacial strength of 3D-C/Cs than that of 2D-C/Cs [42, 43]. Even 2D-C/Cs exhibit notch insensitivity to some extent [37, 44, 45]. Thus, complete notch insensitivity can be expected for 3D-C/Cs [40].

2.2. *Thermal properties*

The advantages of C/C composites also reside in their high thermal conductivity [3, 46, 47] and low coefficients of thermal expansion (CTEs) [3, 48–50]. A typical CTE of a C/C composite in the axial direction of the fiber ranges from -1.5×10^{-6} to zero 1/K at room temperature. This low CTE of C/C composites is maintained at temperatures over 2000°C, as typically shown in Fig. 3 [49]. In this figure, in-plane, out-of plane, and matrix CTEs are shown for a C/C composite with cross-ply lamination, and are denoted by α_L, α_T and α_m, respectively. When the C/C composites are joined with other materials, such as metals, this extremely low CTE of α_L causes a huge thermal mismatch strain.

The thermal conductivity of C/C composites varies considerably depending on the quality of the carbon fiber [3, 46]. The highest conductivity can be obtained

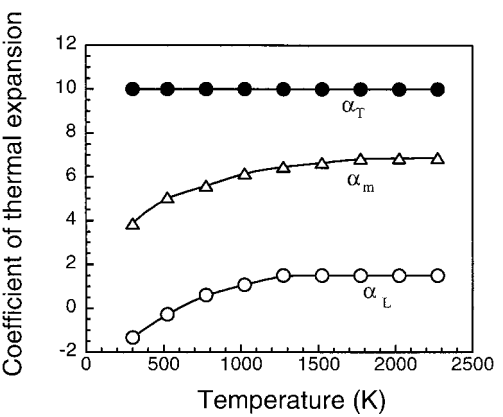

Figure 3. Temperature dependence of thermal expansion coefficients in a unidirectionally reinforced C/C composite in the fiber direction α_L and transverse direction α_T and its matrix α_m [26].

using pitch-based fibers with high heat-treatment temperatures. Conventional C/C composites have intermediate conductivity [26, 49], which is nearly the same as a carbon fiber reinforced polymer matrix composites. However, the highest conductivity of C/C composites is much higher than that of high conductivity metals [3, 23, 51]. These excellent thermal properties make C/Cs highly resistant to thermal shock [3].

2.3. High temperature oxidation

The most serious problem encountered in C/C composites is their low oxidation resistance. In order to improve their oxidation resistance, a coating is often applied on the surfaces of C/Cs. Figure 4 [10] compares the mass loss rates of bare and SiC-coated C/C composites. As this figure shows, the SiC-coating considerably lowers the mass loss rate of the C/C composite. However, this improvement is not sufficient for the ATREX application. The coating on a C/C composite is usually applied at an elevated temperature, exceeding 1000°C. Thus, during cooling from the coating treatment temperature to room temperature, many cracks appear in the coating due to thermal mismatch strains between a coating material and the C/C composite [10, 11]. Through these cracks, oxidation still proceeds. Hence, a glass-based material is usually over-coated on a ceramic coating to seal the cracks [52]. A

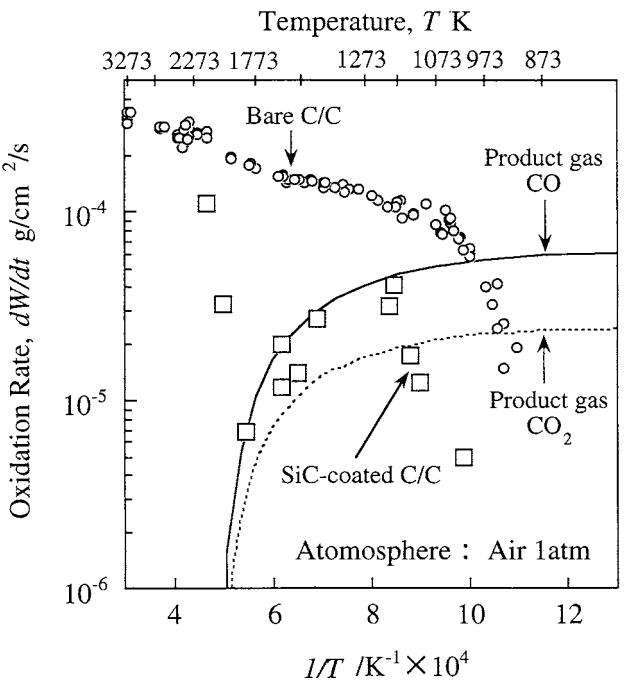

Figure 4. Mass loss rates, dW/dt, of bare and SiC-coated C/C composites due to oxidation. The solid and dashed lines represent numerical results using diffusion model [10, 11] under the assumption that the resultant gas by oxidation reaction is CO or CO_2, respectively.

silicon carbide, SiC, coating over-coated with vitreous crack sealant is now believed to be the most promising. However, it is useful only over short periods and in a temperature range up to about 1700°C [8, 10] due to evaporation of the glass sealant. The glass crack sealant should be liquid in a temperature range suitable for oxidation protection, because the coating cracks vary in width with temperature [52]. Owing to this requirement, the evaporation temperature of the glass sealant inevitably becomes rather low [52]. Consequently, complete suppression of oxygen ingress by diffusion through the coating cracks in a long term is extremely difficult even at rather low temperatures [8]. The SiC coating is oxidized to form a thin, stable SiO_2 film on the coating surface at a temperature range lower than 1700°C under atmospheric pressure. However, over 1700°C, 'active oxidation' occurs in the SiC coating under atmospheric pressure, as shown in the left hand side of Fig. 4, where the SiC coating continuously evaporates in the form of gas phase SiO [11, 53–55].

The turbine disk should be protected against hydrogen at temperatures under 1500°C. The reaction rate of hydrogen with carbon or SiC is about 10^2 to 10^3 times lower than that of oxidation [56]. Thus, the SiC coating is sufficient for a short time usage of the turbine disk.

3. TURBINE DISK

3.1. Design of turbine disk

The tip-turbine structure to be formed using a 3D-C/C has a shape shown in Fig. 5. Since C/C composites are the only materials that have superior mechanical properties at temperatures higher than 1500°C [1–3], the utilization of C/C composites is regarded as an indispensable factor to attain a flight speed of Mach 6 [39]. At this speed, the turbine disk rotated up to 440 m/s, and the strength

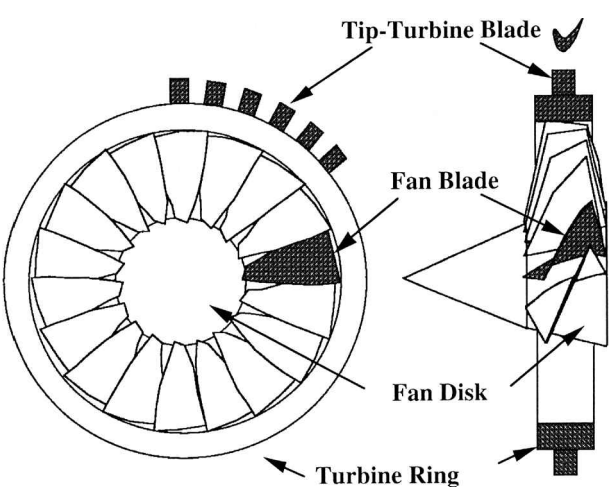

Figure 5. A tip turbine structure for the ATREX engine.

required for a C/C composite at this maximum speed has been estimated to be 350 MPa. Since the high stress caused by centrifugal force in the disk is induced only in the circumferential direction [39, 57], a high volume fraction of reinforcing fiber should be loaded in this direction. A tensile strength higher than 800 MPa was confirmed to be attainable using a 3D-C/C having fiber volume fractions in x, y, and z directions, 40%, 10%, and 5% [31]. Thus, using a r-θ-z reinforced 3D-C/C disk, we can easily satisfy this strength requirement.

3.2. High speed rotation tests

High speed rotation tests have been carried out to explore problems associated with high speed rotation. Another aim of the rotation tests was to clarify the vibration behavior related to rotational imbalance inherent to the C/C disks. Figure 6 represents a schematic illustration of the utilized rotation burst tester driven by air turbines, which has a maximum rotation speed of 100 000 r.p.m. In this tester, telemeters and cameras are installed to measure strain distributions and to take photographs of fracture initiation in rotating disks, respectively. During rotation tests, the test chamber was evacuated by a rotary pump.

The rotational tests were carried out on various annular C/C disks having different reinforcing patterns, 2D or 3D reinforcement, varying ratios of inner and outer diameters, and various notch lengths. These tests verified that the fracture criteria established by static tests are also applicable to the disk even in rotational burst tests [57], and that the required rotational speed for the ATREX application is attainable using a 3D-C/C [58]. Typical model disks made of 3D-C/Cs are shown in Fig. 7.

During the rotation burst tests of the 3D-C/C disks, micro-fractures and the resulting fragment fly-outs were observed at much lower rotational speeds than that of the total fracture [58, 59]. A large number of the fragment fly-outs induced vibration due to rotational imbalance of the disk [59], which is fatally harmful

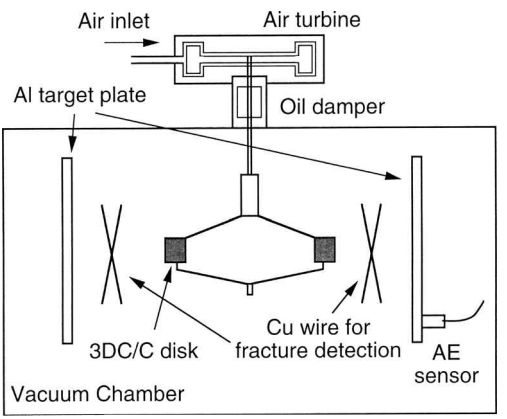

Figure 6. A schematic drawing of the spin burst tester and fracture detection set-up.

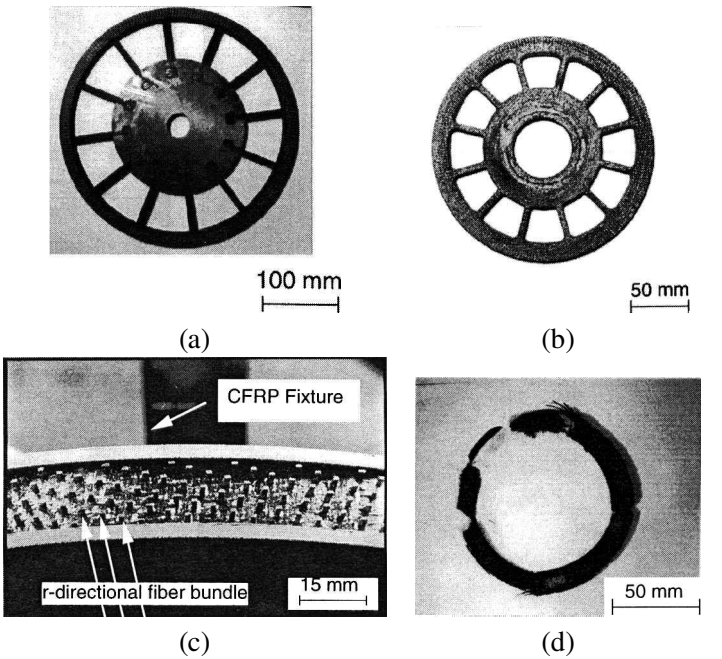

Figure 7. Simplified models of a turbine disk made of 3-dimensionally reinforced C/C composites. (a) Joined structure composed of an outer ring, simplified fans, and inner disk. (b) Monolithic structure. (c) Peripheral surface of a ring specimen after initiation of fly-out phenomenon, in which fiber bundles in the radial direction protrude. (d) Ring specimen after spin-burst.

to the ATREX engine. The clearance between the blade tips and shroud should be set lower than 0.2 mm for production of high rotational power. Vibration of large amplitude might make the blades come in contact with the shroud and result in fracture of the blades. This type of severe micro-fractures was not observed in 2D-C/C discs. This is due to the coarse fiber texture adopted in the 3D-C/Cs (using thicker fiber bundles; 12 000 to 36 000 filaments/bundle) compared with 2D C/Cs and their tendency to possess weaker bundle interfaces [40, 42]. Detailed discussion of this fly-out behavior is given in reference [58], which includes analysis and effective measures to prevent the fly-out phenomenon.

4. HEAT EXCHANGERS

4.1. Design and processing

According to a preliminary calculation, a heat exchange area of 10 m^2 is required to effectively operate the expander cycle in a 40 mm diameter ATREX model [17, 18]. To realize this large heat exchange area, in addition to a conventional insert-type exchanger, it was decided that the walls of the combustion chamber and the plug nozzle needed to be utilized for heat exchangers. The wall type and the insert type heat exchanger now under discussion are schematically shown in Figs 8a

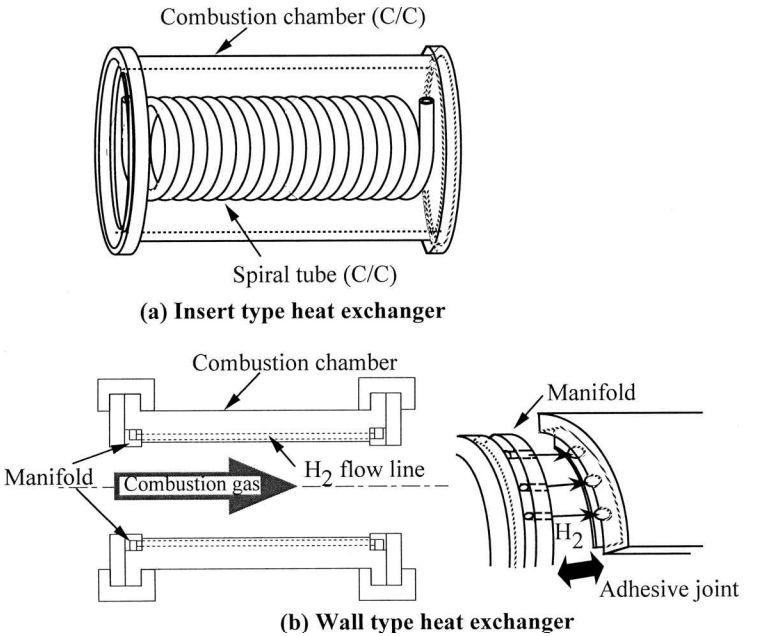

Figure 8. Heat exchangers made of C/C composites under development. (a) Spiral heat exchanger to be set in a combustion chamber. (b) Cylindrical heat exchanger utilizing the wall of a combustion chamber.

and 8b, respectively. Since heat resistance beyond 1500°C is partly required for the materials used in the heat exchangers, C/C composites are experimentally applied in high temperature regions. The primary difficulty in these applications is how to form 3D-C/Cs into the complex shapes of the heat exchanger. The hydrogen gas within the ducts of the heat exchangers possesses a maximum pressure of 40 atm, whereas inside and outside of the combustion chamber, combustion gas and air have pressures of 10 and 1 atm, respectively. Hence, the duct walls and combustion chamber must sustain a maximum pressure difference of 39 atm at a temperature of 1500°C.

The heat exchanger formed in the wall of the combustion chamber is composed of a cylinder containing many duct holes and manifolds, and is fabricated by the processes shown in Fig. 9. This heat exchanger is made of a r-θ-z-reinforced 3D-C/C with fiber volume fractions of $V_{f\text{-}r} = 20\%$, $V_{f\text{-}\theta} = 20\%$, $V_{f\text{-}z} = 3\%$. The manifolds are mounted at the inlet and outlet portions of the combustion chamber. They distribute the fuel H_2 to the ducts of the heat exchanger, and gather and send it to the turbine. In the preform of the combustion chamber shown in Fig. 9(1), 90 copper tubes with an outer diameter of 5 mm were inserted to form the ducts for the hydrogen flow. Copper tubes were used because copper does not chemically react with carbon even at elevated temperatures. The copper tubes were set at 3 mm distances from the free surfaces in order to satisfy the required gas leakage level of 3%. This preform was fabricated first by piercing CFRP rods of 0.8 mm diameter

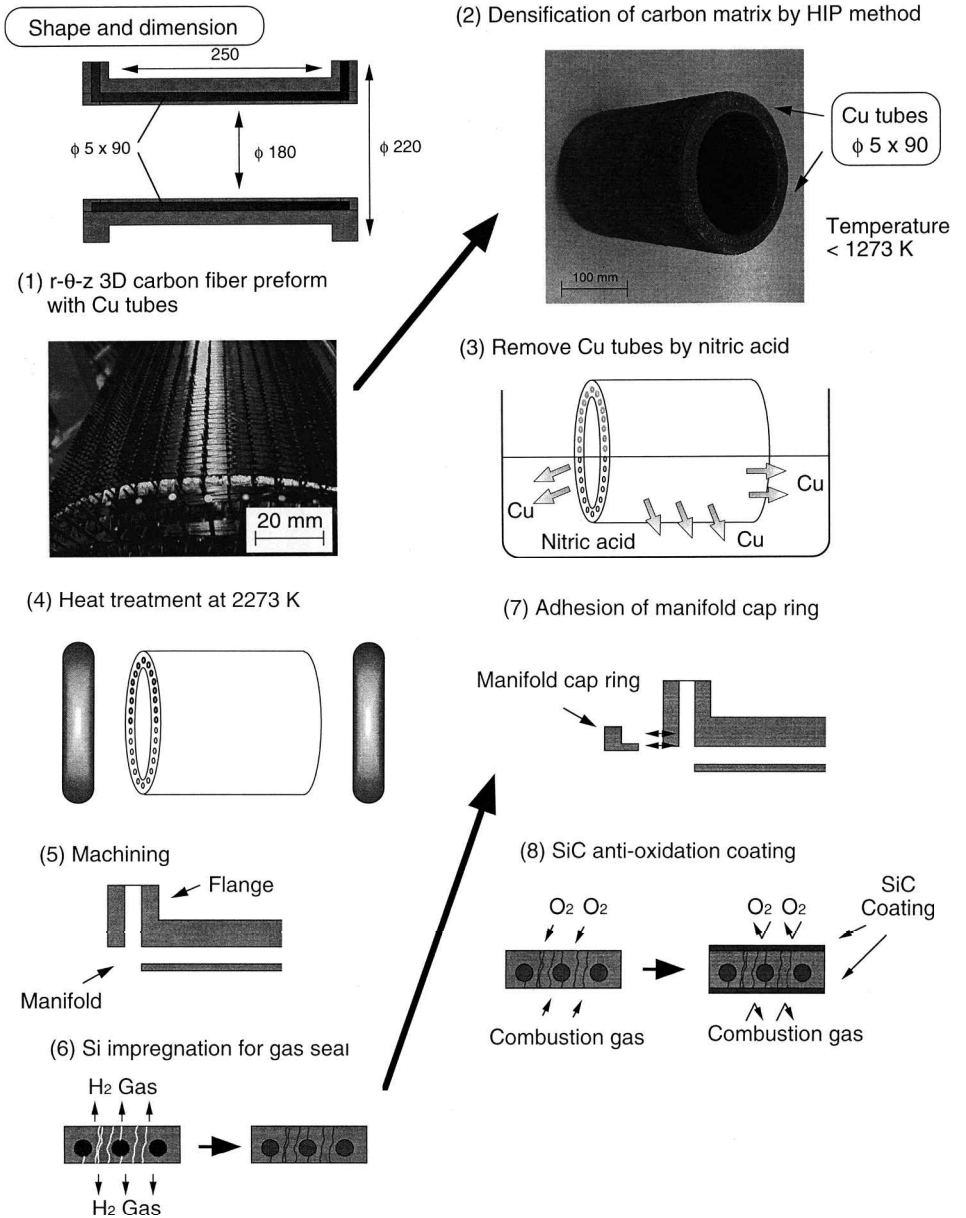

Figure 9. Schematic drawings illustrating a fabrication process of a wall-type heat exchanger.

on a thickly polyurethane-coated mandrel, and then placing θ and z fiber bundles between the pierced rods using filament winding technique. The preform was then infiltrated with phenolic resin, followed by carbonization of the resin at 650°C. The resultant porous 3D-C/C was densified by 4 cycles of hot isostatic pressing until achieving a density of 1.45 g/cm^3. The HIP treatment was performed at a

low temperature of 650°C in order to avoid melting and large deformation of the Cu tubes. The density of 1.45 g/cm^3 might be too low for structural application, but this density is convenient for a Si infiltration treatment for the prevention of gas leakage. This treatment will be discussed later. Next, the copper tubes were chemically dissolved with nitric acid. The resulting 3D-C/C was then heat-treated at 2000°C and carbon-bonded to the manifold.

The above-mentioned process has been completed. The next process shown in Fig. 9(6) is Si infiltration into the 3D-C/C. This process is aimed at the minimization of gas leakage through the exchanger and is performed at 1600°C. The infiltrated Si almost completely occupies the space of open defects in the 3D-C/C and chemically reacts with carbon in the 3D-C/C to form SiC. Finally, a SiC coating and vitreous over-coat is to be applied on the surfaces of the chamber to prevent oxidation of the 3D-C/C. The glass over-coat evaporates easily, so that the over-coating should be treated periodically after a pre-determined operation time [52].

The main component of the insert type heat exchanger shown in Fig. 8a is the thin curved tube. The thin-walled and curved tube can be processed by the following steps. A carbon fiber reinforced phenolic resin, CFRP, tube is at first formed on a copper tube using the filament winding process. The matrix resin was then carbonized. Next, the resultant C/C-Cu tube was densified by repeating precursor resin infiltration and carbonization at 800°C. After that the copper tube is dissolved with nitric acid. Finally, the graphitization process will be performed at 2000°C. The principal difficulty involved in the insert type heat exchanger is joining it strongly to the combustion chamber.

4.2. Key technologies

In addition to design and fabrication technologies, there exist several key technologies which must be established for the production of the heat exchangers. These topics will be briefly reviewed below.

4.2.1. Bonding. The bonding between C/C composites is to be used, for example, between the wall-type heat exchanger and the manifold. The heat exchangers are to be used at high temperatures. Thus, high temperature capability is also required of the bonding material. As a bonding material, carbon and SiC were examined. Carbon bonding is expected to have a high temperature capability exceeding 2000°C, and SiC bonding is expected to result in stronger bonding.

Carbon bonding was performed by the procedure shown in Fig. 10 [60]. The bonding strength between cross-ply C/Cs was evaluated by means of the double-notched compression method [60, 61]. Figure 11 shows the bonding strength and interlaminar strength of the substrate C/C as a function of temperature. As this figure shows, bonding strength as well as interlaminar strength is enhanced with temperature increase. The principal factor for this improvement was shown to be the evaporation of absorbed water [61], and this effect was generally observed in carbon materials [62, 63].

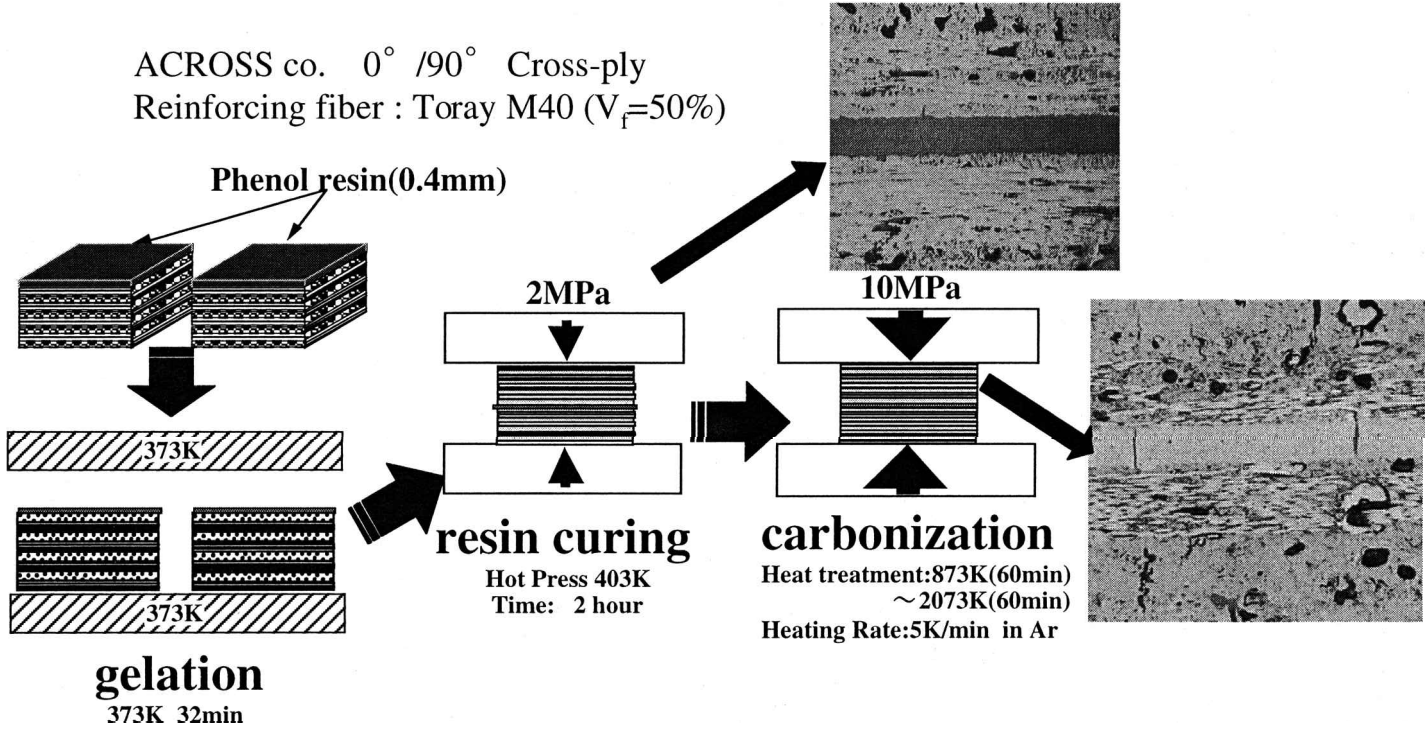

Figure 10. An explanatory diagram of the resin-carbonization-bonding process.

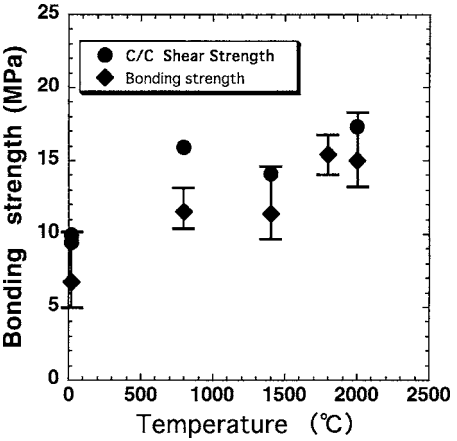

Figure 11. Temperature dependence of bonding strength between C/C composites using carbon adhesive and interlaminar shear strength of the C/C composite.

SiC bonding has a strength of 20–30 MPa, and it has been confirmed already that the bonding strength also improved with temperature increase [64]. Thus, SiC bonding is useful especially in the case in which high bonding strength is required. SiC bonding was executed by placing a Si sheet between polished C/C plates under a pressure of 10 MPa at 1600°C. Under elevated temperatures, Si reacted with carbon in the C/C plates to form SiC. The pressure required at high temperature limits the applicability of SiC bonding. As an alternative method, the following two-step procedure was examined; (1) C/Cs were bonded by carbon, (2) the carbon-bonded C/C was impregnated with Si. This process can be executed without simultaneous application of pressure and high temperature. This method was shown to be effective not only in obtaining high bonding strength but also in the minimization of gas leakage through the bonding layer.

4.2.2. Oxidation. Recently, the authors have developed a new concept regarding the coating deposited on C/C composites [65, 66], which involves a multi-layered SiC/carbon coating composed of submicron-thick layers. It is well known that when the coating becomes thinner than a critical value, coating cracks are suppressed [65–67]. The concept advanced by the present authors involves the alternate stacking of two coating materials with thicknesses lower than the critical values. In this coating, one of the coating materials has to be of a large critical thickness. In the present case, carbon has a critical thickness of about 6 μm. Coating cracks can, then, be completely eliminated as demonstrated in Figs 12a and 12b, where the white layers are SiC and the black layers are carbon [65]. Note that the substrate C/Cs in these photographs are inclined in order to enlarge the CTE of the substrate in the in-plane direction. In the case of Fig. 12a, each coating thickness is thinner than the critical values, but in case (b) the SiC layers are thicker than the critical value. A Si_3N_4/BN multi-layered coating is under development for

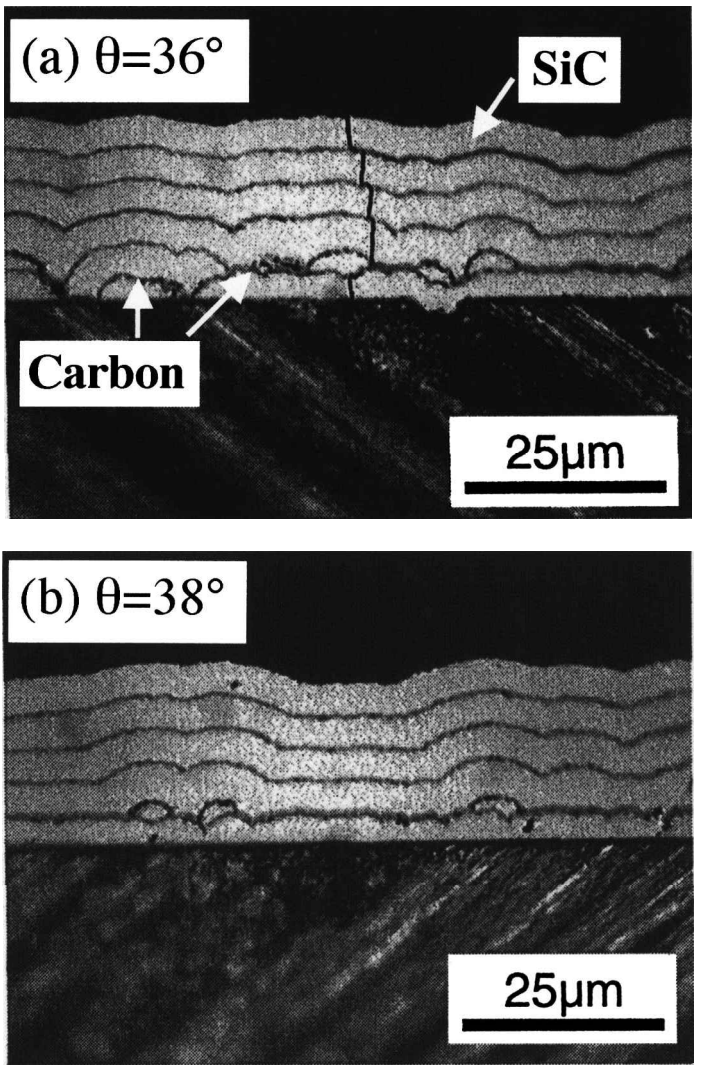

Figure 12. Cross-sectional views of SiC/C multi-layered coatings applied on unidirectionally reinforced C/C substrates inclined the fiber direction in order to change thermal expansion in the horizontal direction. Coating cracks appeared in a 36°-inclined substrate but not in a 38°-inclined substrate. This result demonstrates that crackless coating can be obtained by reducing the thermal mismatch strain between the coating and the substrate.

application to the heat exchangers. Silicon nitride and boron nitride were chosen for this coating, because the critical thickness of the $Si_3N_4 > 1$ μm, is estimated to be much thicker than that of SiC, 0.2 μm, and BN is more oxidation-resitant than carbon.

4.2.3. Gas leakage. C/C composites usually include plenty of pores and cracks as shown in Fig. 13a for a cross-ply laminated C/C. Thus, gas easily passes through

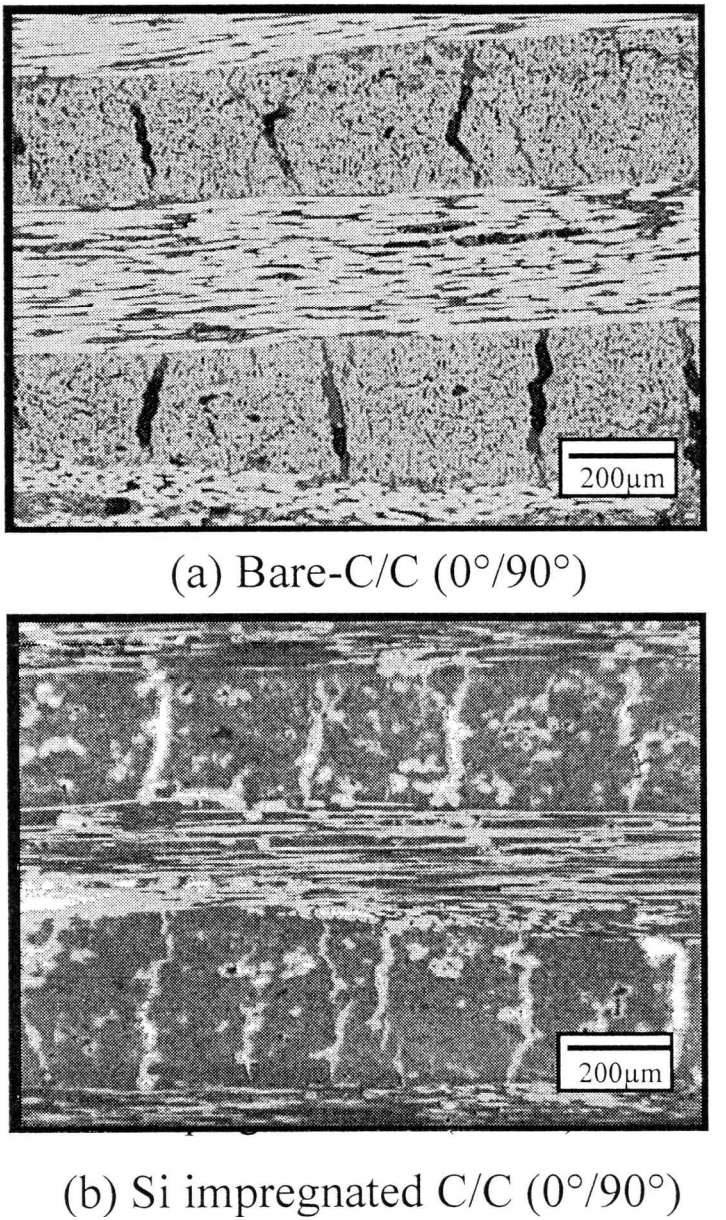

Figure 13. Cross-sections of C/C with cross-ply lamination before (a) and after Si infiltration (b).

C/Cs if no countermeasures are adapted. The ATREX system requires a heat exchanger leakage of less than 3% of the total hydrogen gas [17–19]. However, non-treated C/Cs leak a greater amount of gases than that, as shown in Fig. 14 in which the 3% gas leakage level is indicated by the dashed line. Gas leakage occurs mainly through open pores and cracks. Thus, the gas leak rate strongly depends on

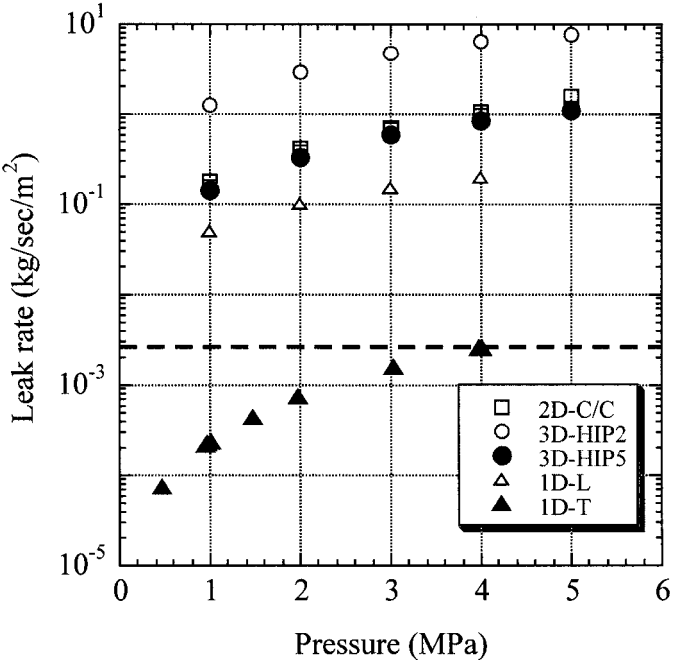

Figure 14. Nitrogen gas leak rates of various bare C/Cs as a function of gas pressure. 0/90; bare cross-ply laminate, 3D-HIP2; 3D-C/C with 2 cycles of HIP-treatment, 3D-HIP5; 3D-C/C with 5 cycles of HIP-treatment, 1D-L; unidirectionally reinforced C/C in the fiber axis direction, 1D-L; unidirectionally reinforced C/C in the transverse direction.

the microstructure of the composites. To prevent gas leakage, two counter-measures were examined. The first examined was Si infiltration into pores and cracks in a C/C composite [68, 69]. This treatment was performed at 1600°C, and most of the impregnated Si was converted to SiC with volumetric expansion [67–73]. The pores and cracks are then almost sealed, though small cracks are newly formed, as shown in Fig. 13b. By this treatment, the gas leak rate was lowered by three orders of magnitude and became lower than that for the ATREX requirement for a 3 mm C/C plate, as shown in Fig. 15 [74, 75]. Exploring further improvements, a refractory metal, Ni, was thinly plated on the surface of the C/C. The Ni coatings were applied using two procedures, electro- and electroless processes, indicated in the figure by Ni-plating and electroless Ni, respectively. The electro-plated Ni tended to include large pin-holes, but electroless plating did not. Thus, electroless plating completely suppressed the leakage. However, the electroless plating is effective under low temperature environments less than 1000°C and under low-pressure differences. When the pressure difference between the both surfaces becomes high, the plating tends to debond from the substrate C/C due to the pressure. Similar leakage problems have been recently discussed by several authors but in different situations [76, 77], for example in the development of a hydrogen rocket tank for use at cryogenic temperatures.

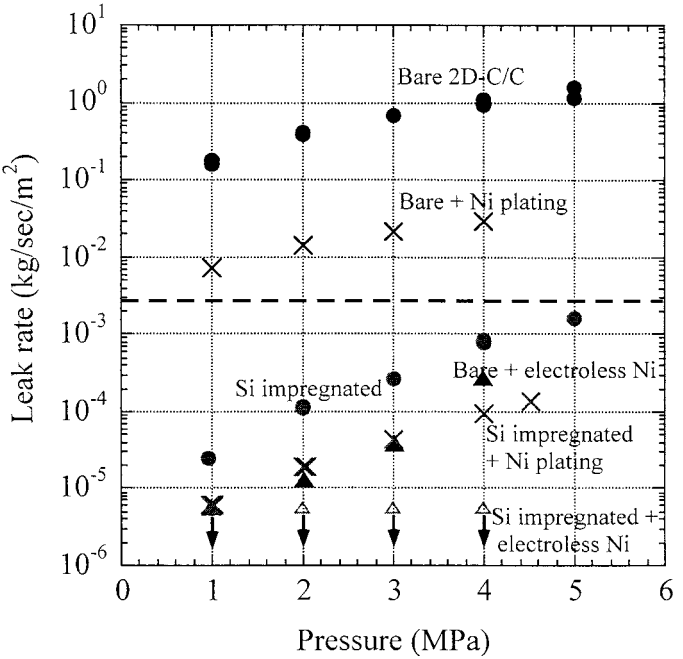

Figure 15. Nitrogen gas leak rates of various cross-ply laminated-C/Cs (2D-C/Cs) a s a function of gas pressure. Bare 2D-C/C; bare cross-ply laminate, Bare + Ni plating; Ni plated on 2D-C/C by electro-process, Bare + electroless Ni; Ni plated on 2D-C/C by electroless-process, Si impregnated; 2D-C/C with Si impregnation treatment, Si impregnated + Ni plating; 2D-C/C with Si impregnation treatment applied Ni electro-plating, Si impregnated + electroless Ni; 2D-C/C with Si impregnation treatment applied Ni electroless-plating.

5. PLUG NOZZLE

Figure 16 schematically shows the plug nozzle for the ATREX engine. This nozzle is connected to the combustion chamber at the cowl. The plug is supported by the two struts. The combustion gas flows through the space between the plug, and the cowl and mobile skirt. The movement of the skirt makes an optimum outlet gap, which varies with flight speed and altitude (environmental pressure). The temperature of the sharp end of the mobile skirt is estimated to be higher than 2000°C due to high temperature gas flow. This region is cooled by gas flow supplied by the 45 holes of 3 mm in diameter.

The cowl and the mobile skirt were fabricated using 3D-C/Cs. The holes for the ejection of cooling gas were formed using the Cu resolving technique employed in the wall-type heat exchanger. The 3D-preforms for struts and plug are now being fabricated. Near net shape 3D-preforms of the struts are difficult to weave. Consequently, the struts were determined to be divided into simple elements, as shown in Fig. 17, which can be formed with 2-dimensional in-plane reinforcement by, for example, the filament winding process. All the elements thus formed are then arranged into the final shape. Finally, thin CFRP rods were pierced in order to

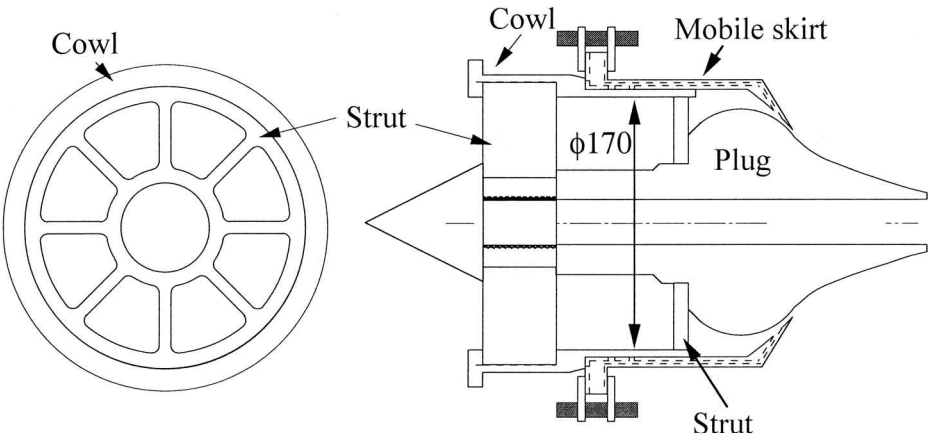

Figure 16. A schematic drawing of the plug nozzle.

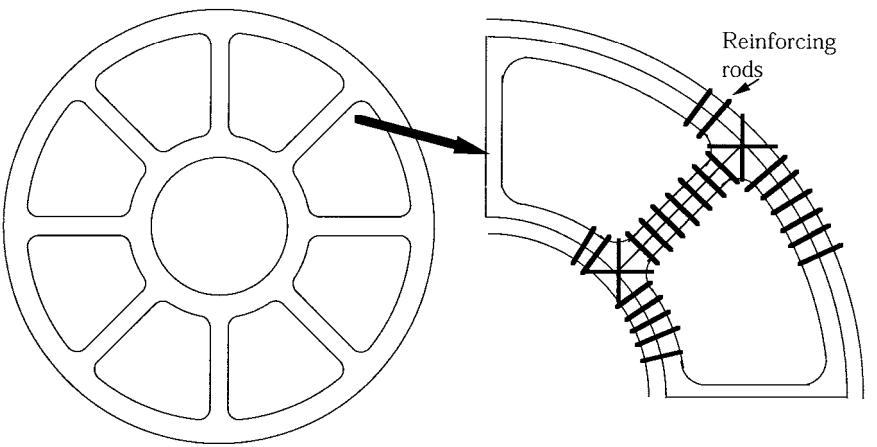

Figure 17. A schematic drawing illustrating the reinforcing pattern of the struts. Thick short lines represent thin rods for the reinforcement in the thickness direction. The rods are made of carbon fiber reinforced phenolic resin matrix composite.

join the elements and to reinforce them in the thickness direction, as schematically illustrated in the right hand figure.

6. MISCELLANEOUS

6.1. Joining

As mentioned above, C/Cs have extremely low CTE. Hence, when the C/Cs are joined to other materials, high residual thermal stresses tend to be induced. In particular, in large structures, thermal mismatch strain might accumulate to develop large stress in the vicinity of the joints. To avoid this thermal stress problem, structures to relieve the mismatch strain must be developed. This problem is

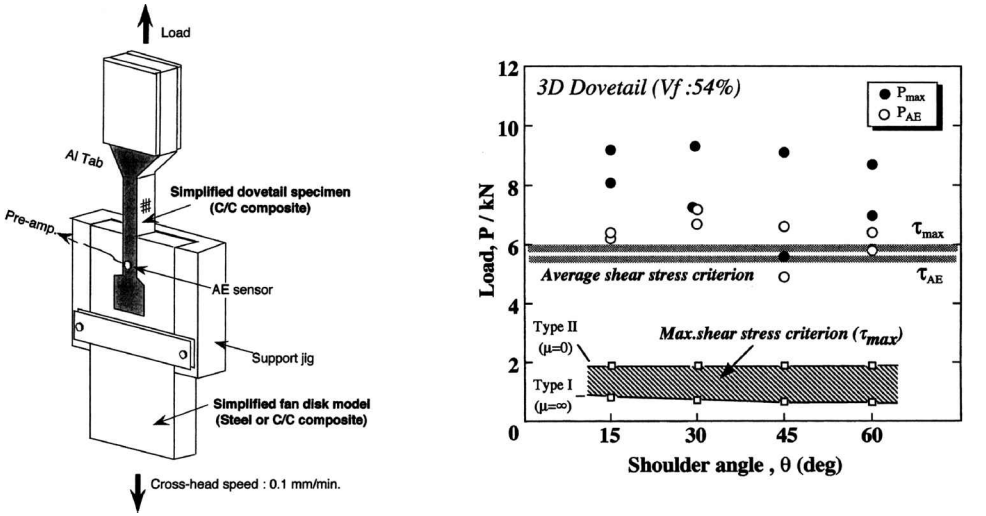

Figure 18. Comparison of experimental results and predictions on load-bearing capabilities of 3-dimensionally reinforced dove-tail joints with various shoulder angles. The predictions are based on average stress criterion calculated from the fracture load divided by the load sustaining area.

presumed to be most serious and important for C/C applications. Thus, this should be the next most important research focus.

Several methods of achieving a strong mechanical joining between C/Cs have been discussed. These include pin joint [78, 79], dove-tail joint [80, 81], and screw joints. 3D-C/Cs have extremely low shear strength compared with tensile strength. Hence, the joint strengths of the 3D-C/Cs tend to be determined by shear strength. Figure 18 [81] shows maximum load P_{max} and initial damage load P_{AE} of a 3D-C/C fabricated by the resin-char method. This figure indicates that the initial damage of the dove tail joint observed when the average shear stress (load divided by load-sustaining area) reached the corresponding value τ_{AE} obtained by shear tests.

6.2. Pipe fabrication

In the expander cycle, the fuel H_2 moves to the heat exchangers, runs through them, and finally arrives at the turbine. Between the intake, heat exchangers, and turbine, the fuel moves in tubes. For these fuel transfers, heat resistant tubes are required. In the discussion of the insert type heat exchanger, it was indicated that pipes can be fabricated by C/C composites. Problems associated with these tubes might involve joining them with engine components. In regard to the C/C tubes, a trade-off study is underway for three types of pipes, (1) a C/C pipe with Si infiltration; (2) C/C formed on a glassy carbon pipe; and (3) a glassy carbon tube. For the improvement of oxidation resistance, SiC is to be coated on the surfaces of these pipes. An optimum pipe structure is sought from the view points of weight saving, minimizing gas leak, and mechanical reliability.

7. CONCLUDING REMARKS

For the last 10 years, the present authors have been investigating C/C composites, with the aim of applying C/C composites to components of the ATREX engine. This feasibility study on C/C composites summarized the recent results of the authors and their coworkers. This ATREX engine project includes not only the turbine disk, heat exchangers, and plug nozzle discussed here, but also the air-intake and miscellaneous components. It is proposed that this project will be scaled-up and the construction of more realistic small scale models made of C/C composites will officially start in the fiscal year 2003. Though these goals constitute great challenges, their achievements will provide valuable information regarding the practical applications of high temperature composite materials in severe environments.

Acknowledgements

This study was financially supported in part by a grant-in-aid for basic science (Grant No. 11305047) from the Ministry of Education, Science, Sports, Culture and Technology of Japan. The authors would like to thank many students and colleagues for their help in the discussion, experiments, and calculations relating to the ATREX project.

REFERENCES

1. G. Savage, *Carbon-Carbon Composites.* Chapman and Hall, London (1993).
2. C. R. Thomas (Ed.), *Essentials of Carbon-Carbon Composites.* Royal Society of Chemistry, Cambridge (1993).
3. E. Fitzer and L. M. Manocha, *Carbon Reinforcements and Carbon/Carbon Composites.* Springer Verlag, Berlin (1998).
4. J. D. Buckley and D. D. Edie (Eds), *Carbon-Carbon Materials and Composites.* NASA Reference Pub. 1254 (1992).
5. D. L. Schmidt, K. E. Davidson and L. S. Theibert, Unique applications of carbon-carbon composite materials (Part One), *SAMPE J.* **35**, 27–39 (1999).
6. D. L. Schmidt, K. E. Davidson and L. S. Theibert, Unique applications of carbon-carbon composite materials (Part Two), *SAMPE J.* **35**, 51–63 (1999).
7. D. L. Schmidt, K. E. Davidson and L. S. Theibert, Unique applications of carbon-carbon composite materials (Part Three), *SAMPE J.* **35**, 47–55 (1999).
8. J. R. Strife and J. E. Sheehan, Ceramic coating for carbon-carbon composites, *Am. Ceram. Soc. Bull.* **67**, 369–374 (1988).
9. K. L. Luthra, Oxidation of SiC-containing composites, *Carbon* **8** (7-8), 649–653 (1987).
10. T. Aoki, H. Hatta, Y. Kogo, H. Fukuda, Y. Goto and T. Yarii, Oxidation behavior of SiC-coated C/C composite, *Trans. Japan Soc. Metal.* **62**, 404–412 (1998) (in Japanese).
11. H. Hatta, T. Aoki, Y. Kogo and T. Yarii, High temperature oxidation behavior of the SiC-coated C/C composites, *Composites, Part A* **30**, 515–520 (1999).
12. H. Hatta, M. Kashimura, Y. Kogo and S. Somiya, Oxidation and strength degradation of SiC-coated C/C composites, *Trans. Japan Soc. Mech. Eng. Part A* **64**, 246–252 (1998) (in Japanese).

13. S. Kobayashi, S. Wakayama, T. Aoki and H. Hatta, Oxidation behavior and strength degradation of CVD-SiC coated C/C composites at high temperature in air, *Adv. Composite Mater.* **12**, 169–181 (2003).
14. H. Kuczera *et al.*, FESTIP system activity-overview and status, in: *Proc. IAF*, 98-V.3.04 (1998).
15. I. Bekey, SSTO Rocket, A practical possibility, *AIAA Aerospace America* **4** (7), 32 (1994).
16. M. Maita and H. Kubota, Japanese space plane/RLV programme, in: *AIAA 8th Inter. Spaceplane and Hypersonic System and Tech. Conf.*, Plenary paper, 1998.14. The United States, Europe, and Japan for development of reusable space plane (1998).
17. T. Sato, N. Tanatsugu, H. Kobayashi, H. Hatta, K. Goto, K. Isomura and J. Tomike, Present status of the ATREX engine development toward the flight test; in: *23rd International Symposium on Space Technology and Science*, ISTS 2000-a-12 (2002).
18. T. Sato, N. Tanatsugu, H. Hatta, K. Goto, H. Kobayashi and J. Tomike, Development study of the ATREX engine for TSTO spaceplane, in: *10th International Space Planes and Hypersonic Systems and Technologies Conference*, AIAA-2001-1839 (2001).
19. T. Sato, N. Tanatsugu, T. Kimura and J. Tomike, Countermeasures against the icing problem in the ATREX precooler, in: *51st International Astronautical Congress*, IAF-01-S.5.02 (2001).
20. K. Goto, H. Hatta, M. Oe and T. Koizumi, Tensile strength and deformation of a 2D carbon-carbon composite at elevated temperatures, *J. Am. Ceram. Soc.* (in press).
21. L. M. Manocha, The effect of heat treatment temperature on the properties of polyfuryl alcohol based carbon-carbon composites, *Carbon* **32**, 213–223 (1994).
22. M. Takabatake, Development of petroleum pitch derived high performance C/C composites, in: *8th Symposium on High Performance Materials for Service Environments*, pp. 273–282 (1997).
23. N. Kiuchi, Y. Ido, Y. Sohda, H. Takashima, T. Sekigawa, F. Takeda, M. Taguchi and K. Enomoto, The mechanical and thermal properties of advanced C/C composites using pitch based carbon fibers, in: *8th Symposium on High Performance Materials for Service Environments*, pp. 297–306 (1997).
24. I. Iwata and O. Otani, Development of advanced C/C composites made of PAN-based carbon fiber, in: *8th Symposium on High performance Mater. for Service Environments*, pp. 387–396 (1997).
25. Y. Kogo, H. Hatta, A. Okura, Y. Obayashi, Y. Sawada and M. Fujikura, Strength and toughness of C/C composite at elevated temperature, *Trans. Tokyo Institute of Polytech.* **17** (1), 50–58 (1994).
26. JUTEM, Durability of high temperature composites at ultra-high temperatures, Research report, NEDO-ITK-9209 (1993).
27. Y. Kogo, H. Hatta, A. Okura, M. Fujikura and Y. Seimiya, Bending and interlaminar shear strengths of C/C composites at elevated temperatures, *Tanso* **166**, 40–46 (1995) (in Japanese).
28. H. Hatta, K. Suzuki, T. Shigei, S. Somiya and Y. Sawada, Strength improvement by densification of C/C composites, *Carbon* **39**, 83–90 (2001).
29. Y. Kogo, R. Sumiya, H. Hatta and Y. Sawada, Examination of strength-controlling factors in C/C composites using bundle composites, *Adv. Composite Mater.* **12**, 137–152 (2003).
30. B. Trouvat, X. Bourrat and R. Naslain, Toughening mechanism in C/C minicomposites with interface control, in: *Extended Abstracts 23rd Biennial Conf. on Carbon, American Carbon Society*, PennState, pp. 536–537 (1997).
31. T. Ikegaki, H. Hatta, K. Goto and H. Hamada, Mechanical properties of three-dimensionally reinforced carbon/carbon composites, in: *Proc. 6th Int. Japan SAMPE*, pp. 533–536 (1999).
32. P. S. Steif, A simple model for the compressive failure of weak banded fiber-reinforced composites, *J. Compos. Mater.* **22**, 818–828 (1988).
33. M. R. Piggot, Compression strength of carbon, glass, and kevlar-49 fiber reinforced polyester resins, *J. Mater. Sci.* **15**, 2523–2538 (1981).
34. A. G. Evans and W. F. Adler, Kinking as a mode of structural degradation in carbon fiber composites, *Acta Metall.* **26**, 725–738 (1978).

35. P. S. Stief, A model for kinking in fiber composites-II; Kink band formation, *Int. J. Solid Structures* **26** (5/6), 563–569 (1990).
36. A. G. Evans and F. W. Zok, Review: The physics and mechanics of fiber-reinforced brittle matrix composites, *J. Mater. Sci.* **29**, 3857–3896 (1994).
37. F. E. Heredia, S. M. Spearing, T. J. Mackin, M. Y. He, A. G. Evans, P. Mosher and P. Brondsted, Notch effects in carbon matrix composites, *J. Am. Ceram. Soc.* **77**, 2817–2827 (1994).
38. L. Denk, H. Hatta, A. Misawa and S. Somiya, Shear fracture of C/C composites with variable stacking sequence, *Carbon* **39** (10), 1505–1513 (2001).
39. H. Hatta, Y. Kogo *et al.*, Conceptual design of turbine disk made of C/C composites for ATREX engine, ISAS Report 85 (1996) (in Japanese).
40. M. S. Aly-Hassan, H. Hatta, S. Wakayama and K. Miyagawa, Comparison of 2D and 3D carbon/carbon composites with respect to damage and fracture resistance, *Carbon* **41**, 1069–1078 (2003).
41. M. S. Aly-Hassan, H. Hatta and S. Wakayama, Effect of zigzag damage extension mechanism on fracture toughness of cross-ply laminated carbon/carbon composites, *Adv. Composite Mater.* **12**, 221–234 (2003).
42. T. Takei, H. Hatta and T. Sugano, Compressive and interfacial strengths of skeletonized tri-axially-reinforced composites, *J. Jpn. Soc. Compos. Mater.* **18** (1), 17–27 (1992) (in Japanese).
43. H. Hatta, T. Takei and A. Mori, Thermo-mechanical properties of three-dimensionally reinforced polymer matrix composites, *Materials System* **10**, 71–80 (1991) (in Japanese).
44. Y. Kogo, H. Hatta, H. Kawada and T. Machida, Effect of stress concentration on tensile fracture behavior of carbon-carbon composites, *J. Compos. Mater.* **32** (13), 1273–1294 (1998).
45. H. Hatta, Y. Kogo, H. Asano and H. Kawada, Applicability of fracture toughness concept to fracture behavior of carbon/carbon composites, *JSME Inter. J., Series A* **42** (2), 265–271 (1999).
46. E. Yasuda, Y. Tanabe, H. Machino and A. Takaku, Thermal expansion behavior of various types of carbon fibers up to 1000°C, in: *Proc. 13th Biennal. Conf. Carbon*, pp. 30–31 (1987).
47. H. O. Pierson, *Handbook of Carbon, Graphite, Diamond, and Fullerenes.* Noyes Publishers (1993).
48. H. O. Pierson and D. A. Northrop, Carbon felt, carbon-matrix composites: Dependence of thermal and mechanical properties on fiber precursor and matrix structure, *J. Compos. Mater.* **9**, 118–137 (1975).
49. H. Hatta, Y. Kogo *et al.*, Thermal properties at elevated temperatures of C/C composites, *Materials System* **14**, 15–24 (1995).
50. H. Hatta, T. Takei and M. Taya, Effect of dispersed microvoids on thermal expansion behavior of composite materials, *Mater. Sci. Eng.* **A285**, 99–110 (2000).
51. J. Takayasu, E. Tsushima and T. Izumi, Thermal properties of C/C composites using matrix precursor containing pitch-powder as the main component, in: *6th Symp. High-Performance Mater. for Severe Environments*, Tokyo, pp. 293–301 (1995).
52. H. Hatta, T. Sotome, Y. Sawada and A. Shida, High temperature crack sealant based on SiO2-B2O3 for SiC coating on carbon-carbon composites, *Adv. Composite Mater.* **12**, 91–104 (2003).
53. W. L. Vaughn and H. G. Maahs, Active-to-passive transition in the oxidation of silicon carbide and silicon nitride in air, *J. Am. Ceram. Soc.* **73**, 1540 (1990).
54. M. Balat, G. Flamant, G. Male and G. Pichelin, Active to passive transition in the oxidation of silicon carbide at high temperature and low pressure in molecular and atomic oxygen, *J. Mater. Sci.* **27**, 697–703 (1992).
55. D. E. Rosener and H. D. Allendorf, High temperature kinetics of the oxidation and nitridation of pyrolytic carbide in dissociated gases, *J. Phys. Chem.* **74**, 1829–1838 (1970).
56. P. L. Walter, F. R. Rushinko and L. G. Austin, Gas reaction of carbon, *Advances in Catalysis* **11**, 133–221 (1959).
57. Y. Kogo, H. Hatta, H. Kawada, T. Shigemura, H. Ohnabe, T. Mizutani and F. Tomioka, Spin burst test of carbon-carbon composite disk, **32** (11), 1016–1035 (1998).

58. K. Goto, H. Hatta, Y. Kogo, H. Fukuda, T. Sato and N. Tanatsugu, Carbon-carbon composite turbine disk for the air turbo-ram-jet engine, *Adv. Composite Mater.* **12**, 203–220 (2003).
59. A. Ogawa, Y. Sofue, R. Hashimoto, T. Morimoto, F. Zhou and M. Yonaiyama, An application study of C/C composites to turbine disk, Extended Abstract of *The 3rd HYPR International Symposium on Japan National Project* (1999).
60. H. Hatta, T. Bando, Y. Kogo, K. Goto and H. Fukuda, Bonding of C/C composites, *Material Systems* **18**, 67–74 (2000).
61. M. Koyama, H. Hatta, H. Fukuda and T. Bando, Strength of carbon bonding between C/C composites at elevated temperatures, in: *Proc. M&P2002 JSME/ASME Joint Conf.* (2002).
62. G. W. Rowe, High temperature strength of clean graphite, *Nuclear Eng.*, 102–103 (1962).
63. T. Maruyama and Y. Nisimura, Effect of absorbed gases on mechanical properties of nuclear graphite, *Tanso* **152**, 98–105 (1992) (in Japanese).
64. W. Krankel, T. Henke and N. Mason, In-situ joined CMC component, in: *Proc. Conf. Ceram. and Metal Matrix Compos.*, San Sebastian (1996).
65. T. Aoki, H. Hatta, T. Hitomi, H. Fukuda and I. Shiota, SiC/C multi-layered coating contributing to the antioxidation of C/C composites and the suppression of through-thickness cracks in the layer, *Carbon* **39**, 1477–1483 (2001).
66. H. Hatta, T. Aoki, T. Hitomi, H. Fukuda and I. Shiota, Suppression of through-the-thickness cracks in SiC coating on C/C composites, *Composite Interfaces* **7** (5-6), 425–442 (2001).
67. J. L. Bauth, Cracking of thin bonded films in residual tension, *Intern. J. Solid Structures* **29** (13), 1657–1675 (1992).
68. M. Tadano, M. Sato *et al.*, Application of C/C composites to the combustion chamber of rocket engine, Part 1 Heating tests of C/C composites with high temperature combustion gases, NAL Technical Report, TR-1264, pp. 3–15 (1995).
69. M. Sato, M. Tadano *et al.*, Application of C/C composites to the combustion chamber of rocket engine, Part 2 Fabrication and evaluation tests of rocket chamber, NAL Technical Report, TR-1268, pp. 1–17 (1995).
70. H. Hatta, E. Sudo, Y. Kogo and I. Shiota, Oxidation behavior and its effect on mechanical properties of Si-impregnated C/C composites, *J. Jpn. Inst. Metals* **62** (9), 861–867 (1998).
71. W. Krenkel, Fiber ceramics for reentry vehicle hot structures, in: *40th IAF*, Malaga, Spain (1989).
72. W. Krenkel and P. Schanz, Fiber ceramic structures based on liquid impregnation technique, *42nd IAF*, Montreal, Canada (1991).
73. T. Ozaki and M. Kume, Pitch-based carbon fiber reinforced SiC composites for space optics, *Adv. Composite Mater.* (submitted).
74. H. Hatta, Y. Nishiyama, T. Bando, K. Shibuya and Y. Kogo, Gas leakage through C/C composites, in: *Proc. US–Japan Conf. Compos. Mater.* (2002).
75. Y. Nishiyama, H. Hatta, T. Bando and T. Sugibayashi, The gas leak analysis in C/C composites, *J. Japan Soc. Aeronautical and Space Science* **50** (587), 483–488 (2002).
76. Y. Morino, T. Ishikawa, T. Aoki, H. Kumazawa and Y. Hayashi, CFRP material characterization testing for the RLV cryogenic propellant tank, in: *AIAA-99-1297* (1999).
77. T. Aoki, T. Ishikawa, H. Kumazawa and Y. Morino, Mechanical performance of CF/polymer composite laminates under cryogenic conditions, in: *AIAA-2000-1605* (2000).
78. H. Hatta, Y. Kogo, T. Asano and Y. Sawada, Strength of pin joints made of C/C composites, *Trans. JSME* **A63** (611), 1586–1593 (1997) (in Japanese).
79. L. Denk, H. Hatta, S. Somiya and H. Misawa, Fracture behavior of multi-holed C/C composites, *Adv. Composite Mater.* (submitted).
80. Y. Kogo, H. Hatta, M. Toyoda, K. Goto and T. Sugibayashi, Strength and fracture behavior of dove tail joints made of C/C composites, *J. JSCM* **24** (6), 222–229 (1998).
81. Y. Kogo, H. Hatta, M. Toyoda and T. Sugibayashi, Application of three-dimensionlly reinforced carbon-carbon composites to dove tail joint structures, *Compos. Sci. Tech.* (submitted).